URTeC: 2892229

Considerations in Azimuthal Processing and Velocity Inversion for Unconventional Plays

Mike Perz*[1], William Keller[2], Victor Kriechbaum[2]; 1. TGS, 2. Enervest Ltd.

Abstract

A tightly-sampled 3D land seismic survey from south central Texas was acquired atop the Austin Chalk near Giddings, Texas in 2015. A test subset of that survey was processed using an azimuth-friendly flow, and subsequent azimuthal velocity inversion (VVAZ) generated interval attributes which showed a remarkably strong correlation to historical gas production. Key elements of the azimuthally-AVO-compliant processing flow used to pre-condition the seismic data include (i) 5D interpolation onto a regularly-sampled set of output azimuth spokes; (ii) post-migration noise attenuation operating piecewise on these spokes; (iii) due care in estimating both the azimuth-variant time-shifts which form the input to the VVAZ inversion, as well as the maximum incident angle restricting the contribution of these time-shifts to the inversion; and (iv) testing the impact of the number of azimuths output from 5D interpolation on the quality of the final azimuthal interval velocity attributes. We posit that these key elements should be routinely incorporated into VVAZ inversion projects for unconventional plays worldwide.

Introduction

The data set under consideration in this paper is a 50 sq. mile test subset of the 710 sq. mile Elli-Walker 3D survey which was acquired in 2015 over a portion of Giddings Field and the eastern extension of the Eagle Ford shale play. This tightly-sampled survey was acquired with 990 ft source line spacing, 1155 ft receiver line spacing, 165 ft shot and receiver group intervals, and an active patch size of 28,875 x 29,935 ft. Natural binning for this survey is 82.5 x 82.5. Nominal CMP fold is 195, and the acquisition yielded a rich sampling of both offsets and azimuths. The zone of interest is between the top of the Austin Chalk and the top of the Buda limestone, an approximately 1000 ft interval encompassing both the Austin Chalk and Eagle Ford formations. At the outset of the project, it was suspected that strong vertical fracturing and/or local anomalies in the in-situ horizontal stress field could place a significant control on hydrocarbon production, and accordingly an effort was undertaken to characterize the interval velocity azimuthal anisotropy using the surface seismic data. Processing was performed within an azimuthally-AVO-compliant framework which seeks to preserve kinematic and amplitude signal variations across both offset and azimuth coordinates. After processing through anisotropic (VTI) pre-stack time migration (PSTM), the data were submitted to VVAZ inversion via the Generalized Dix Inversion (Grechka et al., 1999), a methodology which estimates azimuthal interval fast and slow velocities and fast-velocity orientation (*Vint_fast*, *Vint_slow*, ϕ*_int*, respectively) from their RMS counterparts (*Vrms_fast*, *Vrms_slow*, ϕ*_rms*, respectively). The resulting interval anisotropy maps were compared to production maps and a very strong correlation was observed between production and the estimated VVAZ attributes.

The strong correlation between attribute maps and production data implies that VVAZ inversion holds great promise for optimizing future production in the area, and moreover serves as implicit validation of the processing flows and inversion methodology used to produce the maps. The present work carries two main objectives: first, to discuss

those key elements of the processing and inversion flow which led to the successful outcome and second, to showcase the correlation itself.

Theory and Method

This section examines those key azimuthally-AVO-compliant processing steps and VVAZ inversion steps which we believe had the most beneficial and significant impact on the final attribute map generation.

(1) 5D interpolation and output geometry considerations

Implementation details of 5D interpolation can vary widely, but one common practice (and the one adopted here) is to define the 5D internal computational grid in a mixed Cartesian-polar coordinate system: (i.e., *cmp-x, cmp-y, offset, azimuth*) as recommended by Trad (2009). This choice of computational grid naturally produces a high-quality interpolated set of CMP gathers with regular sampling across both offset and azimuth coordinates. In the present study we simply grouped these CMP gathers, as directly output from 5D interpolation, by their common offset-azimuth indices, and the resulting single fold common-offset-vector (COV) ensembles were in turn input to PSTM. Note that this process of direct grouping into COV's avoids a circuitous approach adopted by many practioners comprising the following steps: (i) interpolation using the above internal computational grid; (ii) casting the interpolated data from (i) onto a surface-indexed grid consisting of a set of finely sampled source and receiver lines; and (iii) performing offset-vector-tiling (OVT) on these surface-indexed data to produce single-fold, azimuth-and-offset-localized data subsets which are in turn input to PSTM. Although this "5D+OVT" approach is suitable for creating the surface-consistent data configurations required for certain imaging methods like reverse-time-migration, it is unnecessary for the Kirchhoff algorithm which is commonly used in azimuthal processing workflows, including the present one (Perz and Cary, 2012).

Figure 1 shows a comparison of both 5D interpolation approaches (i.e, direct COV grouping versus 5D+OVT). The two leftmost panes show different display modes for 5D-interpolated data extracted from our test subvolume after direct COV grouping. Figure 1a shows a migrated common-image-point (CIP) gather in common-azimuth-common-offset ("CACO") mode for which primary and secondary sort keys are azimuth and offset, respectively, while Figure 1b shows data in the transpose "COCA" mode (Figure 1b) for which the two sort keys are reversed. Figure 1c shows some data from a different area (West Texas) created by the 5D+OVT approach in snail gather mode, which is essentially a COCA analog. Note the irregular offset sampling in this snail gather compared to the COCA example in Figure 1b. One advantage of our direct COV grouping approach is that it produces a regular, and finely-sampled, distribution of polar offsets, which in turn permits the ready use of some powerful post-migration noise suppression techniques described in the next subsection. By contrast the irregular offset sampling inherent in the 5D+OVT approach precludes the use of these same denoise techniques without some additional interpolation step.

(2) Post-migration spoke-by-spoke noise attenuation

Returning to Figure 1a, we observed strong organization of multiple energy on each of the six individual azimuth spokes (a single spoke is shown by the green box in the figure), a fact we can exploit by applying traditional Radon multiple attenuation piecewise on each spoke. Though not apparent in Figure 1, in other parts of our test subvolume we observed strong organization of linear noise on each azimuth spoke, paving the way for an analogous spoke-by-spoke 2D f-k filtering strategy (where, crucially, the fine offset sampling precludes spatial aliasing) to attack coherent noise trains (in practice we combine the f-k filtering with an adaptive signal addback scheme to ensure no distortion of primary reflections). Figure 2, excerpted from Cheng et al. (2017), shows the cascaded application of spoke-by-spoke linear denoising and multiple attenuation at a location which exhibits a considerable amount of post-migration residual noise. Figure 2a shows the input COCA gather and Figure 2b shows the final denoised result. Clearly the denoise strategy has worked very well: the underlying signal has been unveiled and exhibits very strong azimuthal variation as evidenced by the pronounced "sinusoidal wobble" at far offsets; moreover, inspection of the underlying noise models (i.e., which were subtracted from the input data) in Figures 2c and 2d show no hint of residual primary signal.

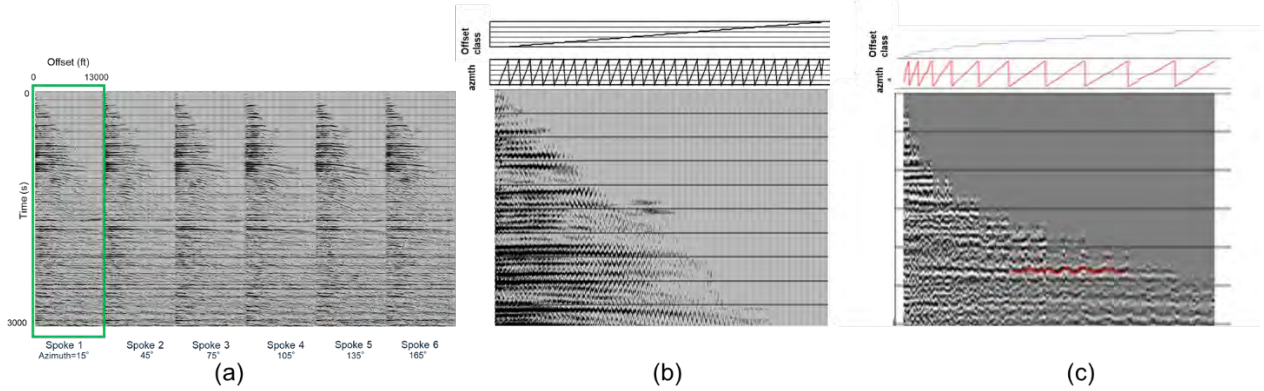

Figure 1: Examples of CIP gathers after 5D interpolation + PSTM: (a) CACO gather of data from our test subvolume created by the direct COV grouping approach with a single azimuth spoke highlighted in green; (b) COCA gather from same data set (but different CIP) created by direct COV grouping approach; (c) snail gather created by 5D+OVT approach from west Texas (excerpted from McCarthy et al., 2016). Seismic data in (a) and (b) is the proprietary property of Seitel Inc.

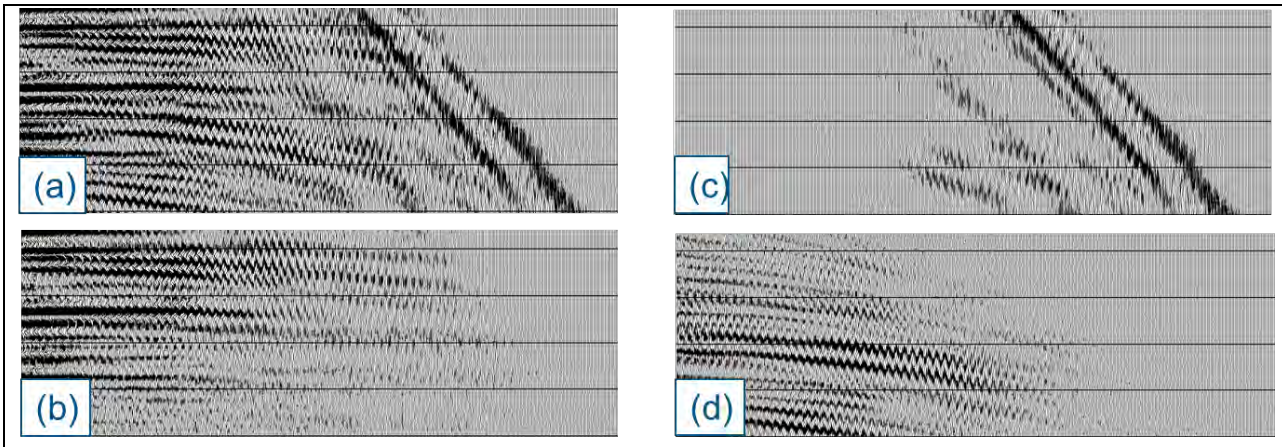

Figure 2: Spoke-by-spoke noise attenuation. (a) input migrated COCA; (b) final denoised COCA after linear noise and de-multiple steps; (c) noise estimated from linear denoise; (d) multiples estimated from de-multiple process. Seismic data is the proprietary property of Seitel, Inc. Figure excerpted from Cheng et al. (2017).

In order to better appreciate the power of this spoke-by-spoke denoising technique, it is important to recognize that the linear and multiple noise trains exhibit significant azimuthal variation themselves (observe the sinusoidal wobble patterns on both noise types in Figures 2c and 2d). The fact that each spoke contains localized azimuth information results in "simplification" in the patterns of these complicated noise trains. This pattern simplification, in turn, helps satisfy the restrictive assumptions underlying the simple processes of f-k filtering and Radon demultiple (i.e, that the noise trajectories lie on perfectly linear and parabolic paths, respectively), ultimately resulting in effective noise attenuation. By contrast a traditional noise attenuation operating across the offset coordinate in an "azimuth-blind" fashion would produce poor results (i.e. because the azimuthal variation in both signal and noise would be smeared in the process, resulting in poor noise removal and signal distortion). Figure 3 illustrates this property of azimuth localization per spoke. The figure compares application of spoke-by-spoke Radon demultiple to its azimuth-blind counterpart commonly used in production 3D land flows today. Note the satisfactory removal of the strong azimuthally-variant multiple energy in the red box in the spoke-by-spoke implementation (Figure 3a, middle), and also note the imperfect removal of that same noise train in the azimuth-blind implementation (Figure 3b, middle). Figure 4 provides additional insight into the efficacy of the spoke-by-spoke approach by showing the Radon domain displays for the two implementations. In the spoke-by-spoke case (Figure 4a—note that only the 75° spoke is shown) the Radon domain shows clear focusing of the offending multiple energy discussed in Figure 3 (red ellipse in the present figure). By contrast the azimuth-blind Radon transform shown in Figure 4b, whose computation

depends only on the offset coordinate, mixes the data across the azimuth coordinate and exhibits relatively poor focusing of this same multiple energy (red ellipse).

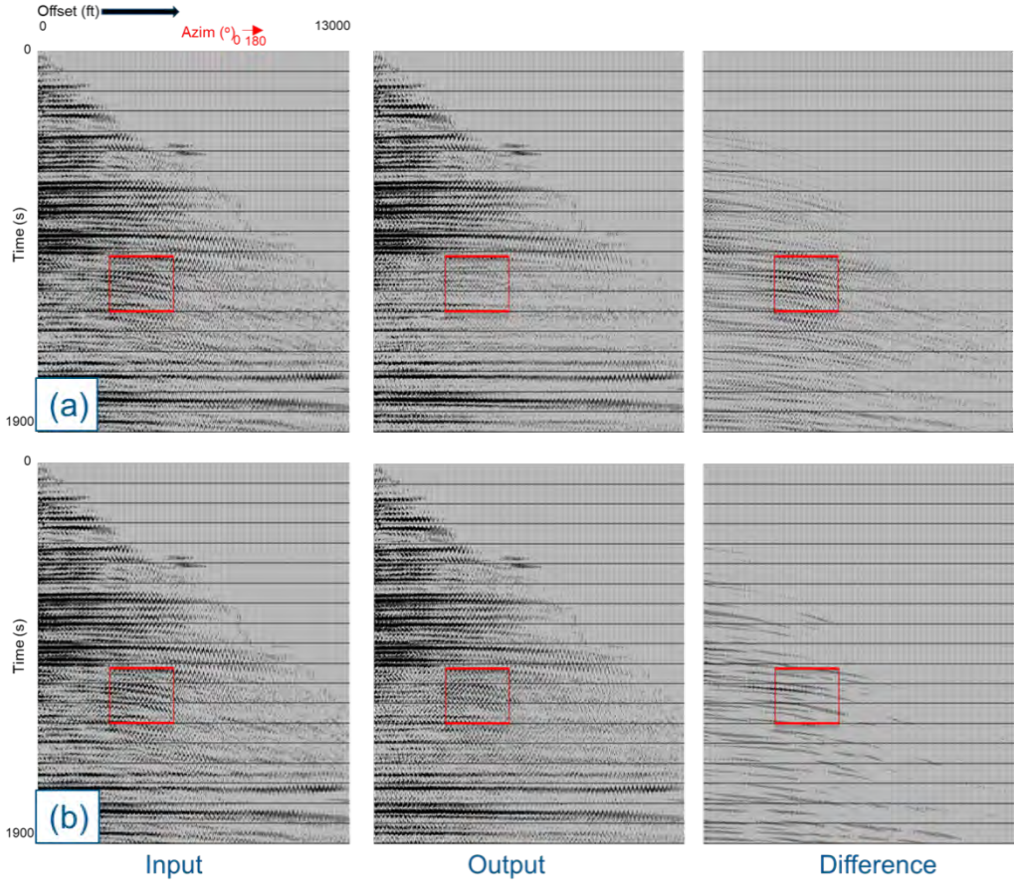

Figure 3: Comparison of spoke-by-spoke and azimuth-blind Radon demultiple. (a) COCA gathers of input (left), output after spoke-by-spoke Radon (middle) and estimated multiple model (right); (b) repeat of COCA gathers of input (left), output after azimuth-blind Radon (middle) and estimated multiple model (right). Seismic data is the proprietary property of Seitel Inc.

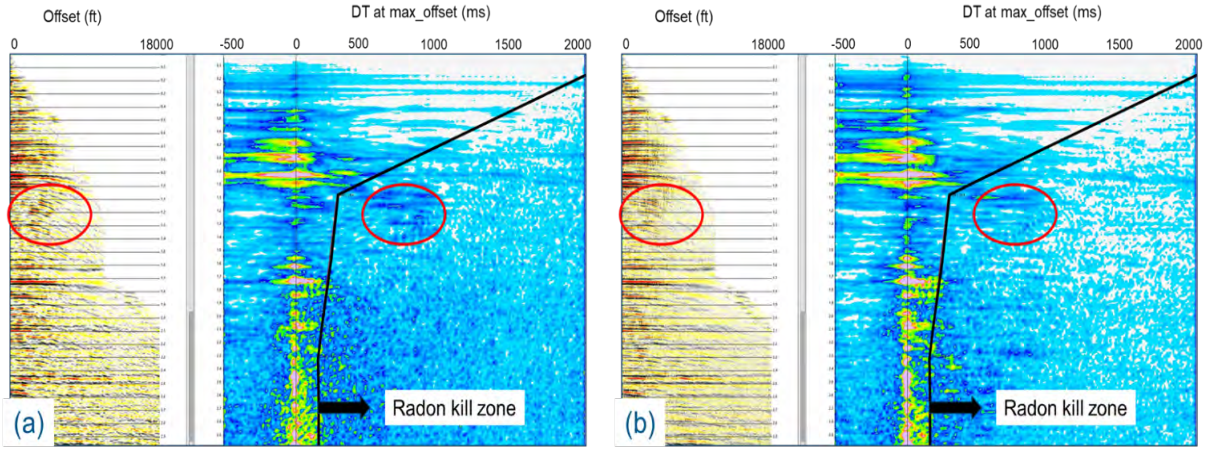

Figure 4: Radon domain comparison of spoke-by-spoke and azimuth-blind Radon demultiple approaches. (a) data from a single spoke at azimuth 75° (left) and corresponding Radon domain plot (right); (b) COCA display of entire gather containing all azimuths (left) and corresponding Radon domain plot (right). COCA in (b) is plotted at 6:1 horizontal compression compared to (a) in order to reflect six-fold data increase. Seismic data is the proprietary property of Seitel Inc.

(3) VVAZ inversion considerations

(i) Time shift estimation

After spoke-by-spoke noise removal as described in the previous section, the migrated CIP gathers were input to an algorithm which estimates the Δt time shifts causing the sinusoidal wobble observed in Figure 2b. Estimation of these Δt's was non-trivial because of the large amount of azimuthal anisotropy present in this data set combined with the fact that this survey captures an uncommonly large incident angle range. While this large angle range ultimately benefits the VVAZ inversion process (because the highly oblique ray angles are very sensitive to the effects of azimuthal anisotropy), it introduces a large disparity between near and far offset waveforms which can bedevil the Δt-estimation process. Figure 5a shows a migrated CIP exhibiting extreme azimuthal anisotropy for which Δt time shifts are estimated via two different approaches. The first approach is the "AVO-projected pilot" technique of Zheng et al. (2008), an approach which honors offset-dependent amplitude effects but not waveform changes. Figure 5b shows the result after first estimating, then applying, the Δt's from this approach (note that a perfect result would imply perfect gather flattening). While the algorithm has done a good job of flattening up to 45°, severe cycle-skipping is observed at the higher angles (blue ellipse). Figure 5c shows the result of applying Δt's estimated via an alternative "sliding window" approach. which explicitly honors offset-dependent waveform changes. Clearly the approach has produced excellent event flattening, even at the highest propagation angles (orange ellipse), and was therefore selected for use in the production run.

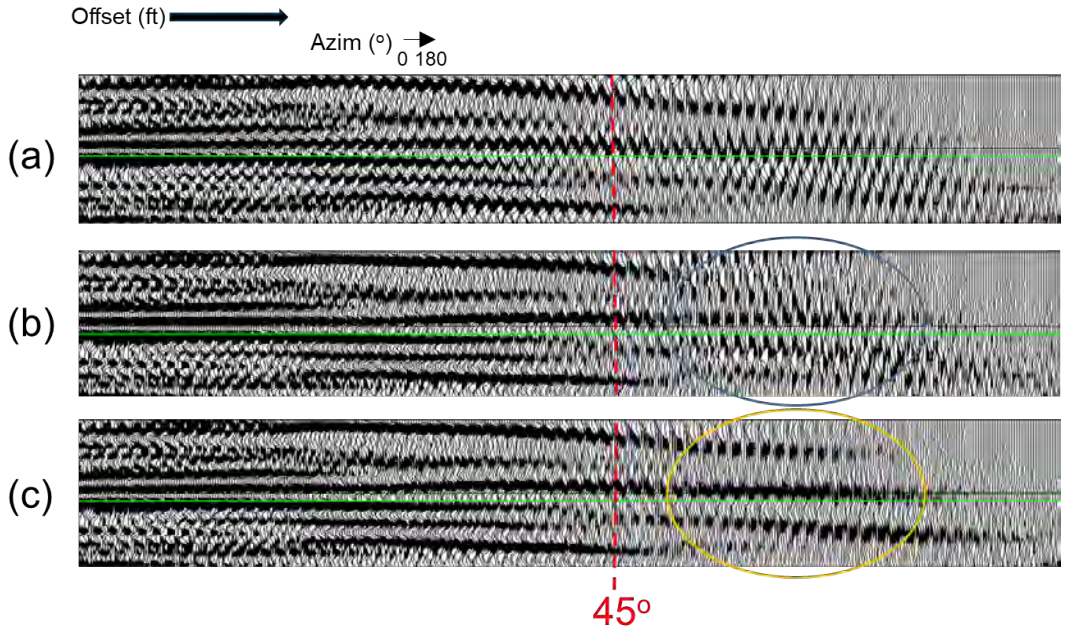

Figure 5: Comparison of Δt time shift estimation approaches. (a) input data (migrated COCA); (b) after flattening with Δt's computed via AVO-projected pilot algorithm c) after flattening with Δt's computed via sliding window approach. Red dashed line shows 45° angle. Seismic data is the proprietary property of Seitel, Inc. Figure adapted from Cheng et al. (2017).

(ii) Maximum angle in RMS parameter estimation

After computation via the "sliding window" approach described in the previous section, the Δt's were input to an elliptical curve-fitting process (Grechka and Tsvankin, 1998) in order to estimate the azimuthal RMS velocity properties *Vrms_fast*, *Vrms_slow*, and ϕ*_rms*,. One important input parameter in the curve-fitting process is the maximum incidence angle for which the Δt's are inverted and its optimal selection proved surprisingly difficult in the present work. Figure 6a shows a final migrated CIP gather in COCA mode, while Figure 6b shows its counterpart after azimuthal NMO correction where the associated azimuthal RMS inversion only considered Δt's corresponding to a maximum incidence angle of 40°. Clearly the wobble associated with mid-range offsets (blue ellipse) is well-collapsed; however, the far offset wobble (orange ellipse) has unfortunately been accentuated, rather than minimized. Figure 6c shows the azimuthal NMO correction based on a 65° maximum inversion angle; in this case the far offset wobble is nicely reduced while the mid-range wobble has been exacerbated. This tradeoff between optimal mid and far offset flattening proved impossible to perfectly manage, and in the end it was decided

that a 60° angle be used in the production run. This decision was largely based on the observation that the downstream-generated VVAZ interval map generated using the 60° RMS inversion gave a better fit to FMI data compared to the 40° case (FMI analysis not shown here)..

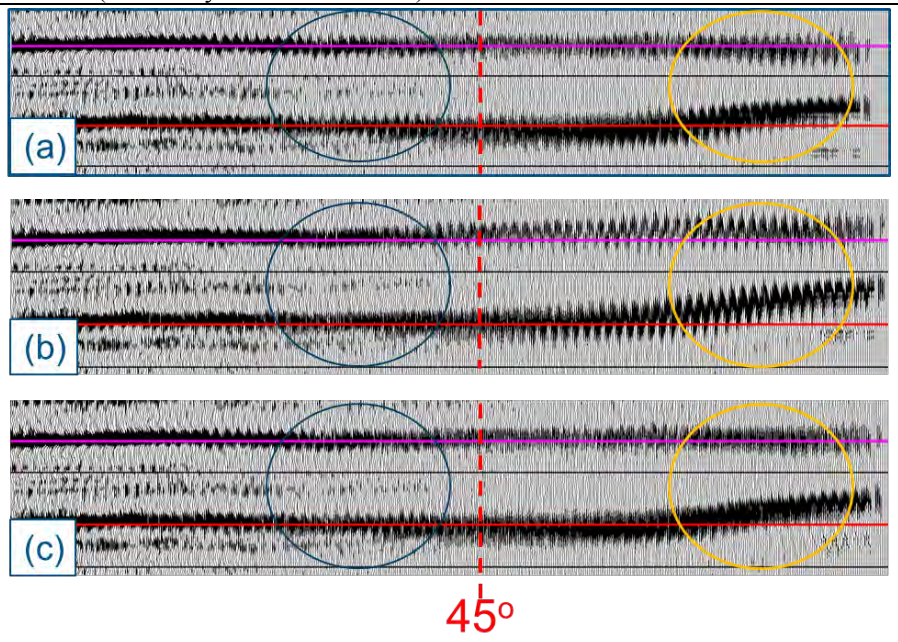

Figure 6: COCA's before and after azimuthal NMO correction. (a) data before correction; (b) after correction via azimuthal RMS property inversion with maximum angle of 40°; (c) same as (b), except a maximum angle of 65° was used. Seismic data is the proprietary property of Seitel, Inc. Figure adapted from Cheng et al. (2017).

While we are unsure of the precise cause of this observed sensitivity of maximum angle to the quality of the azimuthal RMS inversion, one likely explanation is that our elliptical moveout approximation is failing to adequately describe the actual reflection trajectory. There are, in turn, two likely reasons for this failure: first, the elliptical moveout approximation loses its validity at high propagation angles such as those encountered on the far offset traces in the present survey; second, the existence of lateral velocity heterogeneity and/or orthorhombic anisotropy may cause complex traveltime distortions (even at modest propagation angles) which can't be explained by our relatively simple time processing scheme consisting of VTI PSTM plus elliptical moveout correction.

(iii) Impact of number of azimuths

Lynn (2011) showed that the quality of the azimuthal RMS parameter estimates can vary with the number of input azimuths (with reliability improving with increasing number), and, correspondingly, that the number of azimuths may have a profound impact on the quality of the final VVAZ interval estimates. His experimental approach, while scientifically sound, did not consider the effects of 5D interpolation, a relatively new algorithm which introduces a complex interplay between signal-to-noise enhancement and interpolated image quality. In the present work we extended Lynn's study to examine the question of how the number of azimuths output from 5D interpolation (and in turn input to the azimuthal RMS inversion) might impact the quality of the final VVAZ interval parameter estimation. Specifically we considered the same azimuthally anisotropic earth model as Lynn (2011) and we performed forward modeling to create synthetic traces (i.e., containing anisotropic traveltime effects) based on the real survey geometry of the test subvolume. We added random noise to this synthetic data set and submitted the noisy data to 5D interpolation for several trial output-azimuth configurations. Next, for each output-azimuth configuration we estimated Δt shifts, performed the elliptical curve fitting to compute RMS azimuthal parameters, and finally executed the Generalized Dix Inversion to estimate the interval VVAZ parameters. Results from this synthetic experiment were reported in Cheng et al. (2017), with the key finding being that quality of the Generalized Dix Inversion does not improve monotonically with increasing azimuth. In fact, our test revealed that quality actually *degrades* when the number of azimuths is increased to a very large level (20), an observation which is likely due to the fact that 5D interpolation struggles with extreme, and regular, upsampling across any of its coordinates (in this case azimuth).

Next we repeated the above experiment, but this time using real data extracted from the test subvolume. Figure 7 shows the real-data azimuthal interval maps (in this case percentage anisotropy is displayed) for three trial output azimuth scenarios: 6, 10 and 20. All three maps look remarkably similar, and while we don't see any degradation in

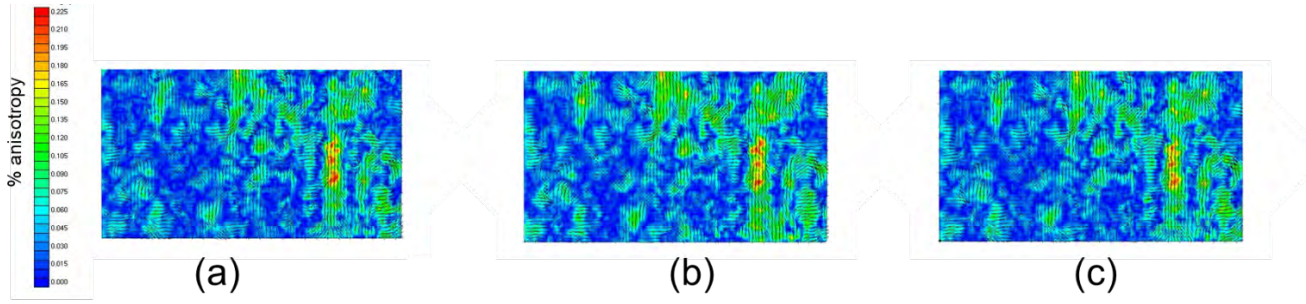

Figure 7: Interval estimates of percent anisotropy extracted from southeast part of test subvolume for three trial output-azimuth configurations . Percent anisotropy is defined as (*Vint_fast -Vint_slow)/ Vint_fast,* and fast direction orientation is indicated by background vectors. (a) 6 output azimuths; (b) 10 output azimuths; (c) 20 output azimuths.

the 20-azimuth result (as was observed in the synthetic case), we note that the 6-azimuth result looks virtually identical to its 10-azimuth counterpart.

Based on the results of this testing, six azimuths were output from 5D interpolation in the production VVAZ inversion run. In addition to producing high-quality inversion output, this 6-output-azimuth scenario offers the added benefit of reducing runtime (where it should be noted that a separate, and relatively expensive, PSTM needs to be run for each output azimuth).

Results

After processing the data and performing the VVAZ inversion based on the considerations discussed in the "Method" section above, the resulting interval attributes were compared to cumulative production at the Austin Chalk level (Figure 8). The map contains a complex symbology whose precise detail is provided in the figure caption. Note the clear visual correlation between the warm colors of the *Vint_slow* attribute (corresponding to relatively slow values of velocity) and high gas production.

Although the azimuth of Vint_fast varies considerably across the survey area, we note that areas of high anisotropy (i.e. long glyphs, corresponding to areas where the azimuth computation is highly reliable) tend to exhibit a stable dominant azimuth of roughly N45ºE. We also note that these areas also tend to be associated with anomalously low Vint-slow values (red colors). We interpret these high anisotropy regions as fairways that exhibit a high degree of natural fracturing oriented parallel to the Vint-fast azimuth. Perhaps not coincidentally, this dominant azimuth direction is parallel to the regional max horizontal compressive stress, perhaps indicating that natural fractures with this orientation may preferentially be more open than fractures oriented less optimally within the regional stress field.

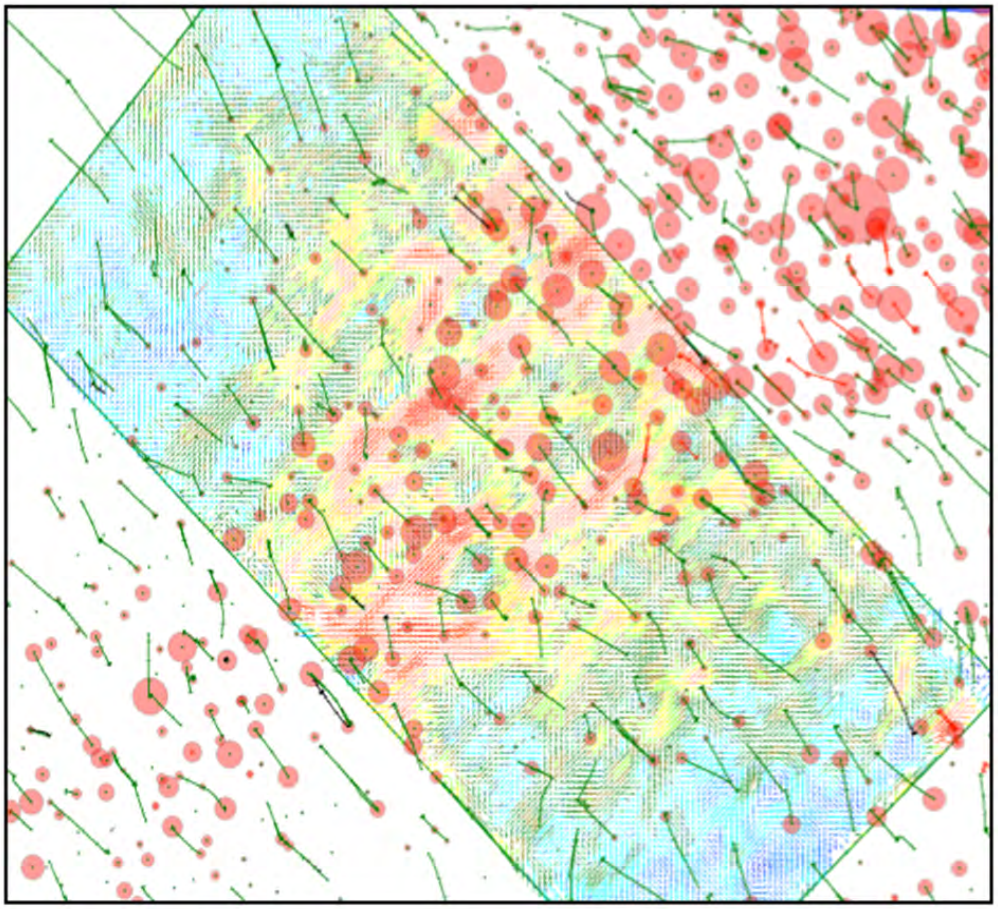

Figure 8: Azimuthal interval velocity anisotropy map with cumulative gas production bubble overlay. The study interval extends from the top of the Austin Chalk to the top of the Buda and thus encompasses the entirety of the Austin Chalk and Eagle Ford formations. The interval velocity attributes are displayed as follows: glyph color = Vint-slow (warm colors are slower than cold colors), glyph length = % Vint Anisotropy, glyph azimuth = Vint-fast azimuth. Figure excerpted from Keller et al. (2017).

Discussion

Our observation that VVAZ attributes exhibit a strong visual correlation to cumulative Austin Chalk production amounts to a success story because it obviously implies that VVAZ holds great promise as a tool for optimizing further drilling. While there are likely several factors influencing our successful outcome, we believe there are two main ones. First, because most of the existing wells in this field are open hole completions that were not hydraulically fractured, the impact of completion overprint appears to be minor, a fact which in turn helps to simplify our interpretation. Second, the Austin Chalk is a very thick and highly anisotropic interval that is ideally suited for this type of azimuthal velocity analysis. In other unconventional plays where VVAZ results appear to be disappointing, the culprit may be lack of strong anisotropy and/or a target interval that is insufficiently thick to create stable results.

Aside from the obvious benefit of revealing a promising tool for optimizing future development, our observation of good correlation between VVAZ attributes and production has the ancillary benefit of validating our azimuthally-friendly processing flow. We recommend that this flow be adopted for future VVAZ projects in other unconventional basins, even in cases where the anisotropy is not as strong and for which we typically don't expect such clear-cut success in VVAZ attribute interpretation.

The time-processing methodology discussed in this paper carries at least two important limitations. First it cannot perfectly account for the effects of rapid lateral velocity variation in the overburden, and second, it cannot perfectly compensate for the effects of orthorhombic anisotropy (i.e, the anisotropy associated with vertical fractures embedded in a strongly-layered background medium). Because both effects are suspected to be present in this data area to some degree, a follow-up study was performed in which our 5D-interpolated data were used as input to an orthorhombic pre-stack depth migration (PSDM). Some uplift was observed relative to the time-domain approach reported here, as discussed in a companion URTeC paper (Hilburn et al., 2018).

Though not shown here, a multivariate analytics model was created using seismic attributes generated from both pre-stack inversion and orthorhombic PSDM. This model was used to generate a production prediction map which gave a high fit to existing production data and which appears geologically plausible.

Conclusions

VVAZ attributes were generated across a 50 square mile subset of the Elli-Walker 3D over Giddings Field. These attributes were observed to exhibit a strong visual correlation to cumulative Austin Chalk production in the area, thereby serving as implicit validation of our processing flow and our VVAZ inversion methodology. Key elements of the processing flow include 5D interpolation onto a set of regularly sampled azimuth spokes as well as spoke-by-spoke noise attenuation. Key elements of our VVAZ inversion include careful attention in time shift estimation, use of a relatively large incident angle in azimuthal RMS property estimation, and outputting a relatively small number of azimuths (6) after 5D interpolation.

Acknowledgements

The authors would like to thank Seitel, Inc., EnerVest, Ltd, and TGS for permission to publish this paper. In addition we would like to thank Walt and Heloise Lynn for many enlightening discussions. Finally, we thank Rene' Mott, Peng Cheng, Femi Ogunsuyi, Frank Meng, and Xinxiang Li.

References

Grechka, V. and Tsvankin, I., 1998, 3-D description of normal moveout in anisotropic inhomogeneous media: GEOPHYSICS, **63**(3), 1079-1092. doi: 10.1190/1.1444386

Grechka, V., I. Tsvankin, and J. Cohen, 1999, Generalized Dix equation and analytic treatment of normal moveout velocity for anisotropic media: Geophysical Prospecting, **47**, 117–148, doi:10.1046/j.1365-2478.1999.00120.x.

Hilburn, G., Pendharkar, A., Keller, W., Mott, R., Jumper, A., Kriechbaum, V., 2018, Unconventional play fracture characterization through orthorhombic depth model building: URTeC Annual Conference.

Keller, W., Mott, R., Jumper, A., Lynn, H., Lynn, W., and Perz, M., 2017, Correlation of azimuthal velocity anisotropy and seismic inversion attributes to Austin Chalk production, a south central Texas case study: 87th Annual International Meeting, SEG, Expanded Abstracts, 3992-3996. doi: 10.1190/segam2017-17778987.1

Lynn, W., 2011, Azimuthal interval velocity uncertainty: 81st Annual International Meeting, SEG, Expanded Abstracts, 279-283. doi: 10.1190/1.3627776

McCarthy, A., Ahmadi, A.B., and Schneider, J., 2016, Advanced seismic processing: a case study on imaging in the Delaware Basin: CSEG Geoconvention

Cheng, P., Perz, M., Ogunsuyi, F., Meng, F., Li, X., Keller, W., Kriechbaum, V., Chasing anisotropy in the Austin Chalk and Eagle Ford shale formations: azimuthal processing challenges and considerations: 87th Annual International Meeting, SEG, Expanded Abstracts,458-462. doi: 10.1190/segam2017-17783411.1

Perz, M. and Cary, P., 2012, 5D interpolation and COV migration: a perfect marriage: CSEG Geoconvention

Trad, D., 2009. Five-dimensional interpolation: Recovering from acquisition constraints: GEOPHYSICS, **74**(6), V123-V132. doi: 10.1190/1.3245216

Zheng Y., Wang, J., and Perz, M., 2008, Pitfalls and tips for seismic fracture analysis: 78th Annual International Meeting, SEG, Expanded Abstracts, 1531-1535. doi: 10.1190/1.3059205